A full quantitative analysis of 18 MV photon beam from 2100 C/D-Varian clinical linear accelerator with and without flattening filter

S.R. Mahdavi[1], M.R. Ay[2], M. Zabihzadeh[3, 4,*], M. Allahverdi[2], M. Shahriari[5], M. Hoseini-Ghahfarokhi[6]

[1]Department of Medical Physics, Iran University of Medical Sciences, Tehran, Iran
[2]Department of Medical Physics and Biomedical Engineering, Tehran University of Medical Sciences, Tehran, Iran
[3]Cancer, Environmental and Petroleum Pollutants Research Center, Ahvaz Jundishapur University of Medical Sciences, Ahvaz, Iran
[4]Department of Medical Physics & Department of Clinical Oncology, Faculty of Medicine, Golestan Hospital, Ahvaz Jundishapur University of Medical Sciences, Ahvaz, Iran
[5]Department of Nuclear Engineering, Shahid Beheshti University, Tehran, Iran
[6] Department of Radiology and Nuclear Medicine, Kermanshah University of Medical Sciences, Kermanshah, Iran.

► *Original article*

*Corresponding authors:
Mansour Zabihzadeh, PhD.,
Fax: *+98 613 333 2066*
E-mail:
zabihzadeh@ajums.ac.ir

ABSTRACT

Background: During intensity modulated radiation therapy (IMRT) technique, theoretically, presence of flattening filter (FF) across the beamline of clinical linear accelerator (linac) is not essential to obtain uniform lateral profiles due to intensity modulation of photon beams by multileaf collimators (MLCs). The aim of this study was to investigate the dosimetrical properties of 18 MV photon beam-Varian linac with and without FF. *Materials and Methods*: All dose measurements were performed on 18 MV, FF mode-Varian 2100C/D linac. The FF and flattening filter free (FFF) modes of linac were modeled by MCNPX 2.4. code. The photon and contaminant electrons spectra, dose rate, present depth doses (PDD), lateral dose profiles, total and collimator scatter factors and out of field doses were calculated and compared with and without FF. *Results:* Removing the FF increased the photon and contaminant electron fluences by factors of 5.48 and 3.94 for a 5 × 5 cm2 field size, respectively. The surface dose increased up to 155%. The flatness of dose profile was disturbed and deteriorated with increase of field size. Despite the dependence of the total scattering factor on field size, the variation of collimator scattering factors was neglected. The out-of-field dose decreased about 81.5 % for a 5 × 5 cm2 field size. *Conclusion:* Removing FF from the linac head increases the dose rate and decreases the out-of-field dose, but the increased skin dose and deteriorated flatness of lateral dose profile are the main disadvantages of the FFF mode.

Keywords: Dosimetry, fattening filter, linear accelerator, Monte Carlo simulation, radiotherapy.

INTRODUCTION

In conventional radiotherapy, X-ray photon beams from the clinical linear accelerators (Linac) must be flattened by flattening filters (FFs) across the applied field to deliver a uniform dose to the target volume at a certain depth of homogeneous phantom. Inserting an iron or copper Gaussian shaped FF across the beam-line results in uniform lateral profiles due to the increase of x-ray attenuation from its sides toward the center. In some complex treatments, special dose distributions (shaped by wedges, blocks, compensators, etc.) are needed to deliver a maximum dose to the target volume and a minimum dose to peripheral

healthy tissues [1].

In more recent techniques such as intensity modulated radiation therapy (IMRT), intensity modulated arc therapy (IMAT), tomoherapy and stereotactic treatments, presence the FF is not necessary due to modulated fluence distribution across the field by dynamic multileaf collimators (MLCs) [2-4]. Some dosimetric properties of different linac models (Varian [5-7], Elekta [8-9] and Siemens [10]) have been investigated for the flattening filter free (FFF) mode. The FF scatters or absorbs the primary photon more than 50%; hence it has an effective role in shaping the spectrum and fluxing the beam. Fix *et al* reported that the FF is the most important component to produce the scattered photons and electron contamination [11]. Dalaryd *et al* found a reduction of 31.7% and 47.6% in scattered photons for the non-flattened beam compared to the flattened beam with energy of 6 and 10 MV, respectively [12]. For the flattened beam, variation of head scattering factor was 6 % for different filed sizes, while it was only 2% for the FFF beam [13]. A considerable increased output factor and decreased average energy of photon were found by Titt *et al.* [7]. O'Brien *et al* and Cashmore *et al* concluded that the time needed to deliver the prescript dose would be decreased by removing the FF from the linac head [2,14]; Some commercial FFF mode-linacs have a dose rate 2-3 times higher compared to the FF mode [15]. Shifting of maximum dose depth toward the shallower depth was reported by Sixel and Podgorsak for the FFF mode [16]. An increase of 7% and 25% in surface dose was reported by Kragl et al for 6 and 10 MV, respectively [17]. An elevated dose of 12% was reported for 6 MV photon beam at water depth of 1 mm [18]. Zefkili *et al* and Lee *et al* reported an interesting reduced dose to the organs located out of field [19-20]. Sixel and Faddegon [21] and Guillerminet *et al.* [22] inspected the reasons for increased surface dose by removing the FF from beam line.

In this study, using the Monte Carlo (MC) calculation by MCNPX 2.4.0 code, the advantages and disadvantages of the FFF mode of 18 MV-Varian 2100C/D linac were investigated in detail compared to the equipped standard linac by the FF.

MATERIALS AND METHODS

Experimental measurement

All dose measurements including depth dose and lateral dose profiles of 18 MV-Varian 2100C/D Linac for the FF mode were conducted using a 0.6 cc Farmer ionizing chamber (PTW Freiburg, Germany) at an IBA Blue Phantom (IBA dosimetry Schwarzenbruck, Germany). The Scanditronix Wellhofer dosimetry *system* and OmnoPro software (version 6.4) were used to measure the ionization. The scanning system had positioning accuracy ≤1mm and reproducibility ≤0.1 mm. Each measurement was repeated three times and its averaged value was reported to ensure the stability of output.

MC calculation

The MC radiation transport code of MCNPX 2.4.0 was used to dose calculation [23]. The modeled linac include the X-ray target, primary collimator, vacuum window, FF, monitor ion chamber, mirror and the upper and lower jaws. The detailed geometry and materials required for accurate modeling of linac head were provided by the explicit data of the vendor. The energy spectrum and lateral spread of incident electron beam on the target (defined by Gaussian distribution) were tuned to reach a good agreement for the present depth dose (PDD) and the dose profile curves between the MC calculation and measurement. The electron and photon cut off energies were set to 0.521 and 0.01 MeV, respectively. To save running time, the phase space (PS) file was calculated at the upstream surface of upper jaws and all photons and electrons were scored. This PS was used to transport particles in all MC calculations.

The photon and contaminant electron fluences per MeV per initial incident electron on the linac target (with energy bin of 0.02 MeV) were calculated in a plane normal to the central axis and in an area equal to applied field size at SSD=100 cm. To calculate the PDDs in water

138

Int. J. Radiat. Res., Vol. 17 No. 1, January 2019

phantom ($50 \times 50 \times 50$ cm^3), a cylinder with a radius of one-tenth of the used field size was defined and divided to scoring cells with 2 mm height along the beam central axis. For beam profile calculations, the cylinder was located at the reference depth vertically to the beam central axis with the voxel thickness of 2 mm. To investigate the change of energy spectra with off axis distance, photon and contaminant electrons energy spectra were scored in spheres (r=0.5 cm) centered on the central axis and 20 cm off-axis distance for the field size of 40×40 cm^2. The collimator scatter factor, S_c, was calculated in an air sphere (r=0.25 cm) at SSD=100 cm, as the ratio of photon Kerma for a given field size to that for the reference field size ($10 ´ 10$ cm^2). The total scatter factor, $S_{c,p}$, as the ratio of photon dose for a given field to the $10 ´ 10$ cm^2 field size was calculated at depth of 10 cm in water phantom at SSD=100 cm. The lateral dose profile curves of the FF and FFF modes at depth of 10 cm were normalized to unity on the central axis. The penumbra was defined as the interval distance between 80% and 20% isodose curves, $P_{80-20\%}$ (mm). The field edge was considered as distance of point with $D_{50\%}$ from the central axis, ($X_{50\%}$, mm). The local dose difference between data of the FF and FFF modes were calculated by equation 1:

Dose differenc = (|dose$_{FF}$ - dose$_{FFF}$|)/dose$_{FFF}$ (1)

All MC programs were processed by the MCNPX code (version 2.4.0) implemented in Pentium IV computer with windows 7 (32-bit Operating System), random access memory (RAM) = 4GB, Intel (R) Core (TM) i5-6300U, central processing unit (CPU) @ 2.4GHz 2.5 GHz. A total of 1×10^8 electron histories were simulated to obtain the PS file (~4 GB). The uncertainties were < 1% and <5% for different lateral distances of the in-field and out –field regions, respectively.

RESULTS

Benchmark of MC model
For the FF mode, an acceptable match was found between the measured and MC calculated PDD and dose profile curves. The incident electron beam was set to the mean energy of 18.1 MeV, Gaussian energy distribution with FWHM of 0.6 MeV and lateral intensity spread with FWHM of 0.1 cm, respectively. The agreement between measurements and calculations was within 1.5 % for depth dose curves in descending part beyond the maximum dose depth and within 2% for lateral dose profiles inside the field. The statistical uncertainty of the calculated PDD curves (1σ) was <1%. The maximum statistical uncertainty was <4.5% for lateral dose profile of the 40×40 cm^2 field size. More details of this modeled linac head could be found in our previous studies [24-25].

Photon spectra
The photon spectra for different field sizes at SSD=100 cm were calculated; only data for $10 ´ 10$ cm^2 field size is shown in figure 1.

For the FF mode, average energy of reached photons to SSD=100 cm decreased from 4.88 to 3.83 MV for $5´5$ cm^2 and $40 ´ 40$ cm^2 field sizes, respectively (table 1); however, removing the FF decreased the average energy of photons from 3.61 to 3.24 MV, respectively. The photon fluence ratio of the FFF mode to that of the FF mode decreased from 5.48 for $5´5$ cm^2 to 1.99 for $40´40$ cm^2 field sizes.

The photon spectra on the central axis of beam and on the field edge of $40 ´ 40$ cm^2 field size were presented in figure 2. For the FF mode, there are more photons with high energy in the central part of field (figure 2a); however, removing the FF did not pronouncedly change the spectra (figure 2b).

Contaminant electrons spectra
The contaminant electron fluence per initial incident electron was tallied and averaged over the surface equal to applied field sizes at SSD=100 cm; only data of 10×10 cm^2 field size is shown in figure 3.

Increasing the field size from $5´5$ cm^2 to $40´40$ cm^2 decreased the average energy of contaminant electrons from 3.79 to 3.18 MeV and from 3.76 to 3.16 MeV for the FF and FFF

Int. J. Radiat. Res., Vol. 17 No. 1, January 2019

139

modes, respectively (table 2). The ratio of electron fluence of the FFF mode to the FF mode was greater for the smaller fields: 3.94 for the 5´5 cm² compared to 1.67 MeV for 40´40 cm² field size.
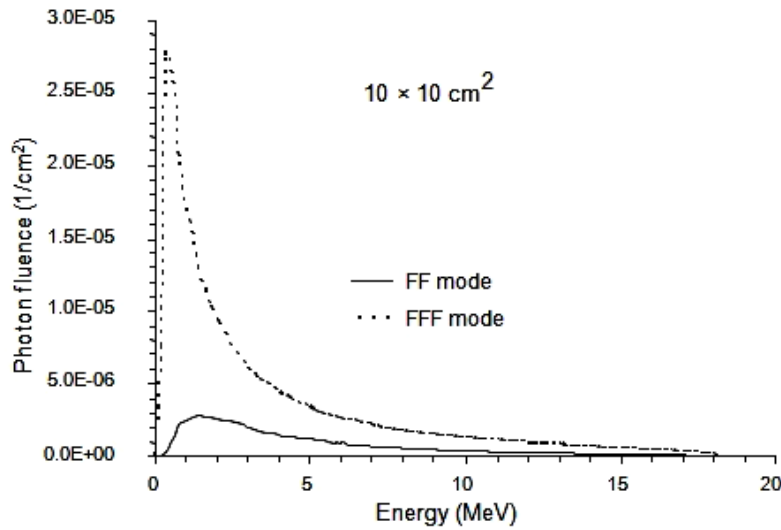

Figure 1. Photon fluences (cm^{-1}) of the FF (solid line) and FFF (dotted line) beams for 10 ´ 10 cm² field size.

Table 1. The average energy, energy of maximum fluence and total fluence of photons.

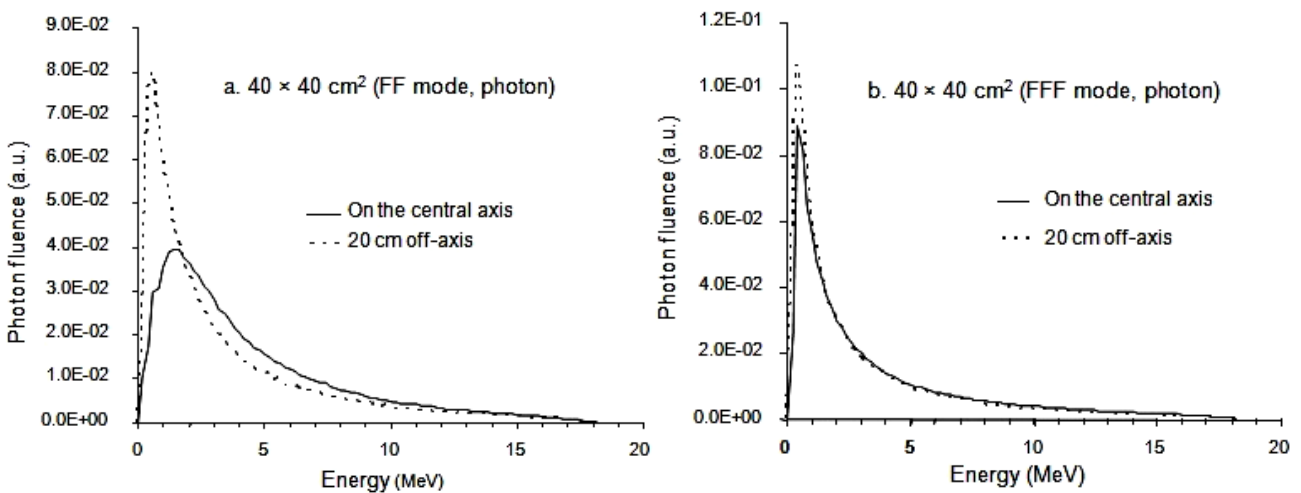| Field size (cm²)	Average energy (MV)		Energy of maximum fluence (MV)		Total fluence (cm^{-2})		
	FF	FFF	FF	FFF	FF	FFF	FFF/FF
5´5	4.88	3.61	1.5	0.3	5.86 ´ 10^{-5}	3.21 ´ 10^{-4}	5.48
10´10	4.72	3.56	1.3	0.3	7.13 ´ 10^{-5}	3.12 ´ 10^{-4}	4.37
20´20	4.41	3.42	0.9	0.3	8.64 ´ 10^{-5}	2.63 ´ 10^{-4}	3.04
30´30	4.05	3.31	0.6	0.3	9.36 ´ 10^{-5}	2.16 ´ 10^{-4}	2.31
40´40	3.83	3.24	0.5	0.3	8.10 ´ 10^{-5}	1.61 ´ 10^{-4}	1.99

Figure 2. Photon fluence spectra normalized per total fluence a. with and b. without the FF for 40 ´ 40 cm² field size; on the central axis (solid line) and on 20 cm off-axis distance (dotted line).
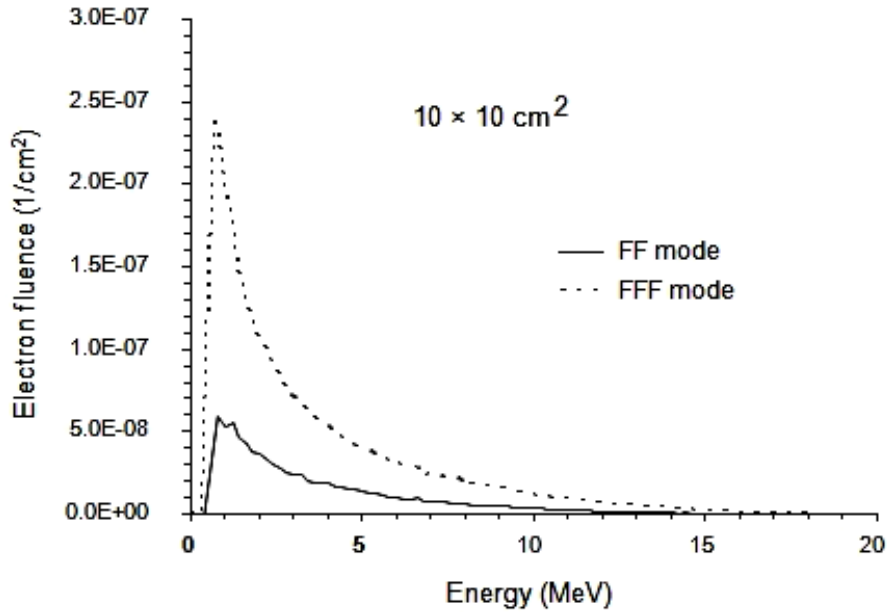
Figure 3. The electron fluences (cm^{-1}) of the FF (solid line) and FFF (dotted line) mode for 10´10 cm^2 field size

Table 2. The average energy, energy of maximum fluence and total fluence of contaminant electrons.

Field size (cm^2)	Average energy (MeV)		Energy of maximum fluence (MeV)		Total fluence		
	FF	FFF	FF	FFF	FF	FFF	FFF/FF
5´5	3.79	3.76	0.7	0.7	5.06 ´ 10^{-7}	2.00 ´ 10^{-6}	3.94
10´10	3.65	3.57	0.7	0.7	9.04 ´ 10^{-7}	2.91 ´ 10^{-6}	3.22
20´20	3.44	3.38	0.7	0.7	1.50 ´ 10^{-6}	3.49 ´ 10^{-6}	2.33
30´30	3.29	3.24	0.7	0.7	1.80 ´ 10^{-6}	3.40 ´ 10^{-6}	1.89
40´40	3.18	3.16	0.7	0.7	1.72 ´ 10^{-6}	2.88 ´ 10^{-6}	1.67

Spectra of contaminant electrons scored on the central axis and 20 cm off-axis distance are calculated for the 40´40 cm^2 field size (only data for the FFF mode is shown in figure 4). The mean energy of contaminant electrons decreased from 3.51 to 3.24 MeV and from 3.32 to 3.17 MeV with and without the FF, respectively.

Present depth dose curves

Present depth dose curves on the beam central axis were computed in water phantom for field sizes of 5´5 cm^2 to 40´40 cm^2 at SSD=100 cm (only data for 5´5 cm^2 field size is shown in figure 5). For a deeper depth beyond the maximum dose depth, the PDDs of the FFF mode were underlined instead of the FF mode while for the buildup region they were located upstream.

The PDD values in depth of 10 cm (D_{10}), depth of 80% dose ($d_{\%80}$) as well as surface dose (D_0) are shown in Table 3. Removing the FF increased the surface dose. The surface dose increased from 26.7% to 61.5% for the FF mode and from 41.5% to 76.3% for the FFF mode. Examining the calculated PDDs showed that removing the FF shifted the depth of maximum dose to shallower depths for smaller fields and moved it to deeper depths for larger fields.

Total and collimator scattering factors ($S_{c,p}$, S_c)

$S_{c,p}$ and S_c are shown in figure 6. Extending the field size increased the $S_{c,p}$ from 0.945 to 1.064 and from 0.951 to 1.050 for the FF and FFF modes, respectively. For the FF mode, S_c increased from 0.963 to 1.031; however for the FFF mode, S_c did not show any significant

Int. J. Radiat. Res., Vol. 17 No. 1, January 2019

141

change.

Dose profile curves

The lateral profiles at a 10 cm depth of water phantom were calculated with lateral dose resolution of 2 mm (table 4). In contrast to the flattened beam, profiles of the FFF mode showed a strong variation across the field that increased with field size.
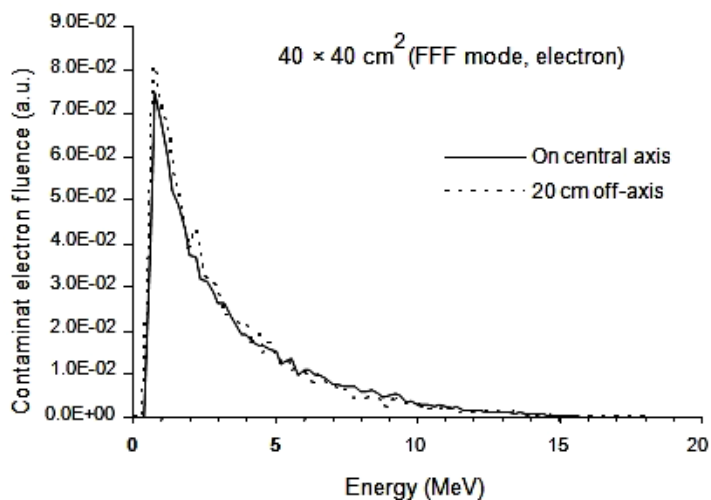

Figure 4. Contaminant electron fluence spectra for the FF and FFF modes. Fluences are normalized to the total fluence.
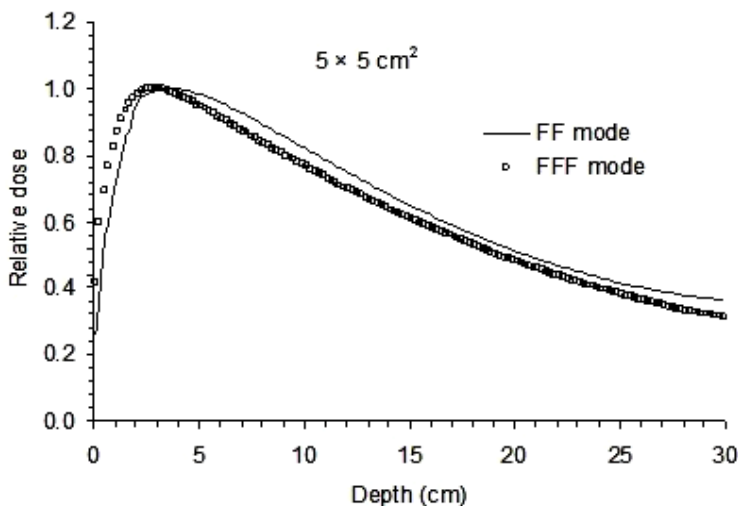

Figure 5. The PDD curves of the FF and FFF modes for different field sizes at SSD=100 cm. Depth doses were normalized to the maximum depth dose. First voxel for scored dose was centered at effective depth of 1mm.

Table 3. PDD in depth of 10 cm (D_{10}), depth of 80% dose ($d_{\%80}$) and surface dose (D_0) for different field sizes at SSD=100 cm.

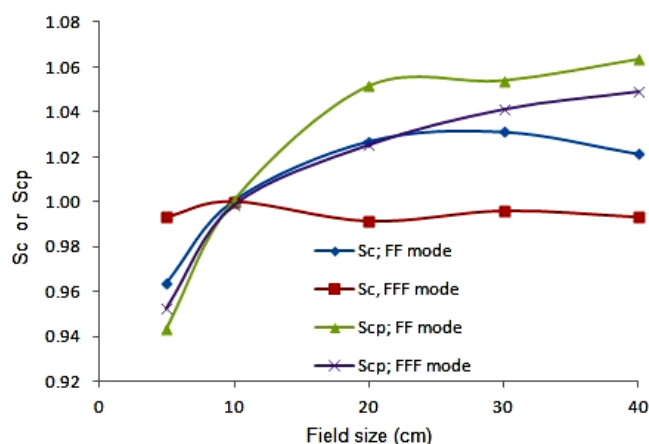| Field size (cm^2)	D_{10}		$d_{\%80}$		D_0	
	FF	FFF	FF	FFF	FF	FFF
5´5	82.2	76.9	10.5	9.1	26.7	41.5
10´10	81.5	77.7	10.3	9.3	39.3	51.4
20´20	80.9	76.6	10.1	8.9	49.8	61.1
30´30	80.1	77.2	9.9	8.9	56.1	71.2
40´40	79.4	77.3	9.7	9.1	61.5	76.3

Figure 6. The total and collimator scattering factors (S_c, $S_{c,p}$) with and without the FF.

Table 4. The penumbra (P80–20% (mm)), field edge (X50%, mm), maximum local difference (%) and difference at 90% of field size (%) of dose profiles for the FF and FFF modes at 10 cm depth of water phantom at SSD=100 cm.

Field size (cm²)	$P_{80-20\%}$ (mm)		Field edge($X_{50\%}$, mm)		Maximum local difference (%)*	Difference at 90% of field size (%)
	FF	FFF	FF	FFF		
10 × 10	7.7	6.9	55.4	53.4	26.5	26.9
40 × 40	9.1	8.0	219.6	102.5	85.1	69.8

* Off-axis distances of 70 and 250 mm were considered to calculate maximum local difference (%) for 10×10 and 40×40 cm2, respectively.

DISCUSSION

Although the photon spectra of the FF and FFF modes have similar shapes, removing the FF severely increases low-energy photons (figure 1). As can be seen from table 1, for the FF mode increasing the field size elevates the scattered photons from field edges and transmitted photons from the thinner parts of the filter and therefore shifts average energy to a lower region (from 4.88 to 3.83 MeV for 5×5 and 40×40 cm², respectively). After removing the FF, lack of scattering and hardening phenomena from filter considerably decreased the average energy of photon compared to the FF beam (table 1), which consequently shifted the maximum dose depth to the shallower depths. Furthermore, the average energy decreased from 4.47 and 3.34 MV for the FF to 3.54 and 2.98 MV for the FFF mode at 0 and 20 cm off-axis distances, respectively. These data are consistent with those reported by Vassiliev *et al*; 4.50, 4.04 and 3.24 MV for the FF mode and 3.34, 2.97 and 2.73 MV for the FFF mode at off-axis distances of 0,

10 and 18 cm, respectively [26]. Sheikh-Bagheri and Rogers [27] reported that the total photons reaching the surface of phantom was 7207 per one million electrons on the target for 10×10 cm² field size (i.e. 7.2 × 10⁻⁵ cm⁻¹), which is in good agreement with our result of 7.13 × 10⁻⁵ (cm⁻¹) for standard linac with the FF. Removing the FF increased the total photon fluence. The ratio of photon fluence for the FFF beam to the FF beam was calculated by Vassilive *et al* as 5.27, 3.72 and 2.01 for field sizes of 10×10, 20×20 and 40×40 cm², respectively, which are comparable with our results of 4.37 3.04 and 1.99 [26]. For clinical applications, this increased dose rate has an interesting probability to decrease the time needed for delivering the prescribed dose to the target volume. Furthermore, shorter treatment time associated with smaller electron and/or neutron contaminant has the potential to decrease the received dose by the health adjacent tissues.

Although the FF eliminates the electrons originating from the upper components, it is the main source for electron contamination [28].

Int. J. Radiat. Res., Vol. 17 No. 1, January 2019

143

Removing the FF allows the transfer of electrons originating from the upper components (that were stopped by FF in the FF mode) and consequently increased the contaminant electron fluence by a factor of 3.94 and 1.67 for 5 × 5 and 40 × 40 cm², respectively (figure 3 and table 2). This undesired increased electron contamination shifts the maximum dose depth to a shallower depth and increases the skin dose. Increased skin dose is a critical drawback of FFF mode that deteriorates the skin sparing property as the greatest advantage of megavoltage beams. Considering the reference dosimetry depths of 5 and 10 cm instead of the maximum dose depth recommended by IAEA-TRS 398 to avoid contaminant electrons is more confirmed for the FFF mode. Our results showed that locating 1mm lead (Pb) filter under the jaws of the FFF mode resulted in a 50% decrease in electron fluence while it is still 61% higher compared to the FF mode without Pb filter. Furthermore, the photon fluence decreased to 60.2%, while it was still 73.8% higher than the FF mode without Pb filter. Therefore, to save the advantage of the FFF mode, compromising the filter thickness is essential to reach maximum decrease in contaminant electrons and minimum decrease in photon fluence, simultaneously.

According to figure 5, depth dose at buildup region is higher for the FFF mode compared to the FF mode while it is underlined for depths beyond the maximum dose depth. As discussed previously, this is expected due to decreased average energy of photons and increased contaminant electrons after removing the FF. Najem *et al* also reported the same patterns for 15 MV photon beam [29]. As shown in Table 3, the relative dose at depth of 10 cm for 10 × 10 cm² field size was 0.777 and the depth of relative dose of 0.8 was 9.3 mm for the FFF modes. From BJR-25 report [30], the same parameters were reported as 0.770 and 9.1 mm for the 15 MV-FF mode linac which are close to our calculated data for 18 MV-FFF mode. This means that in clinical practice to reach the same dosimetric properties of the FF mode with certain energy, photons with higher energy should be selected for treatment with the FFF

mode. Moreover, surface depth dose increased with removing FF as much as 14.8%, 12.1%, 11.3%, 15.1% and 15.25% for 5 × 5, 10 × 10, 20 × 20, 30 × 30 and 40 × 40 cm², respectively. A decrease in the photon energy reduces this skin dose. The increased skin doses of 7.7%, 10% and 13% for 6, 10 [31] and 15 MV [29] for 10 × 10 cm² field size were reported after removing the FF from beam line. Depths of maximum dose of 3.3 and 3.2 cm reported by Vassiliev *et al.* [33] for 18 MV photon beam at field size of 10 × 10 cm² are in good agreement with our data which were 3.33 and 3.12 cm for the FF and FFF modes, respectively. It is worth to note that the drop rate of maximum dose depth was slower for the FFF mode than the FF mode.

As shown in figure 6, for the FFF mode the head scattering factor changes slightly with field size. The total scattering factor changed from 0.945 to 1.064 for the FF mode while it was increased from 0.951 to 1.050 for the FFF mode that are in good agreement with those reported by Kajaria *et al.* [28]. As a result, the smaller change of scattering factor results in lower uncertainties for dose calculation.

Removing the flattening filter causes a significant unflatness in dose profile for the large field sizes. Deterioration of lateral dose profile is a critical obstacle to obtain perfect dose homogeneity in target volume. However, this unflatness is not clinically a concern for the small fields and could not be a considerable obstacle in radiosurgery or tomotherapy techniques. The calculated flatness ranged from 1.20 for 4 × 4 cm² to 2.80 for 40 × 40 cm² (table 4). Vassiliev *et al* reported flatness of 1.20, 1.41, 1.93 and 3.13 for field sizes of 4 × 4, 10 × 10, 20 × 20 and 40 × 40 cm², respectively [26] and Kajarita *et al.* calculated a range of 1.05 to 1.24 for the field sizes of 5 × 5 to 20 × 20 cm² [28], which are in good agreement with our results. Removing the FF reduced the field size about 0.7, 2 and 117 mm for field sizes of 4 × 4, 10 × 10 and 40 × 40 cm², respectively. Consequently the penumbra decreased up to 12.1% (11 mm) for 40 × 40 cm². For the field size of 10 × 10 cm², the penumbra widths of 7.4 and 6.6 mm were calculated by Vasiliev *et al.* (2006), which are comparable with our results of 7.7 and 6.9 mm

for the FF and FFF modes, respectively [26]. Dose at the field edge (at 90% field size) decreased in the FFF mode up to 69.8% for 40 × 40 cm² field size (table 4). Furthermore, doses at depth of 10 cm for 7 and 25 cm off-axis distances from the field edge were 12.1% and 85.1% for 10 × 10 and 40 × 40 cm² field sizes, respectively (table 4). Dose reduction at off-axis distance from the field edge has the potential to reduce dose to the organs at risk located in out-of-field regions which is very interesting to minimize received dose by non-targeted healthy tissues.

CONCLUSION

Removing the FF from linac head has interesting advantages of increased output and decreased out-of-field dose. However, the maximum dose depth shifting to shallow depths and increased skin dose are clinically alarming due to deterioration of the skin sparing as the major advantage of megavoltage beams. The modified FFF beam by Pb electron filter has the potential to improve the small field radiation treatment by clinical linac.

ACKNOWLEDGEMENT

Conflicts of interest: *Declared none.*

REFERENCES

1. Zabihzadeh M, Birgani J, Hoseini-Ghahfarokhi M, Arvandi S, Hoseini SM, Fadaei M (2016) Dosimetric characteristics of 6 MV modified beams by physical wedges of a siemens linear accelerator. *Asian Pac J Cancer Prev, 17: 1685-1689*.
2. O'Brien P, Gillies B, Schwartz M, Young C, Davey P (1991) Radiosurgery with unflattened 6-MV photon beams. *Med phys, 18: 519-521*.
3. Fu W, Dai J, Hu Y, Han D, Song Y (2004) Delivery time comparison for intensity-modulated radiation therapy with/

4. without flattening filter: a planning study. *Phys Med Biol, 49: 1535-1547*.
4. Jeraj R, Mackie TR, Balog J, Olivera G, Pearson D, Kapatoes J, *et al.* (2004) Radiation characteristics of helical tomotherapy. *Med Phys, 31: 396-404*.
5. Kry SF, Howell RM, Polf J, Mohan R, Vassiliev ON (2009) Treatment vault shielding for a flattening filter-free medical linear accelerator. *Phys Med Biol, 54: 1265-1273*.
6. Pönisch F, Titt U, Vassiliev ON, Kry SF, Mohan R (2006) Properties of unflattened photon beams shaped by a multileaf collimator. *Med Phys, 33: 1738-1746*.
7. Titt U, Vassiliev O, Pönisch F, Dong L, Liu H, Mohan R (2006) A flattening filter free photon treatment concept evaluation with Monte Carlo. *Med Phys, 33: 1595-1602*.
8. Mesbahi A, Mehnati P, Keshtkar A, Farajollahi A (2007) Dosimetric properties of a flattening filter-free 6-MV photon beam: a Monte Carlo study. *Radiat Med, 25: 315-324*.
9. Mesbahi A and Nejad FS (2008) Monte Carlo study on a flattening filter-free 18-MV photon beam of a medical linear accelerator. *Radiat Med, 26: 331-336*.
10. Dzierma Y, Licht N, Nuesken F, Ruebe C (2012) Beam properties and stability of a flattening-filter free 7 MV beaman overview. *Med Phys, 39: 2595-2602*.
11. Fix MK, Stampanoni M, Manser P, Born EJ, Mini R, Ruegsegger P (2001) A multiple source model for 6 MV photon beam dose calculations using Monte Carlo. *Phys Med Biol, 46: 1407-1427*.
12. Dalaryd M, Kragl G, Ceberg C, Georg D, McClean B, Wetterstedt S, *et al.* (2010) A Monte Carlo study of a flattening filter-free linear accelerator verified with measurements. *Phys Med Biol, 55: 7333-7344*.
13. Richmond N, Allen V, Daniel J, Dacey R, Walker C (2015) A comparison of phantom scatter from flattened and flattening filter free high-energy photon beams. *Med Dosim, 40: 58-63*.
14. Cashmore J (2008) The characterization of unflattened photon beams from a 6 MV linear accelerator. *Phys Med Biol, 53: 1933-46*.
15. Xiao Y, Kry SF, Popple R, Yorke E, Papanikolaou N, Stathakis S, *et al.* (2015) Flattening filter-free accelerators: a report from the AAPM Therapy Emerging Technology Assessment Work Group. *J Appl Cli Med Phys, 16(3): 5219*.
16. Sixel KE, Podgorsak EB (1994) Buildup region and depth of dose maximum of megavoltage x-ray beams. *Med Phys, 21: 411-416*.
17. Kragl G, af Wetterstedt S, Knäusl B, Lind M, McCavana P, Knöös T, *et al.* (2009) Dosimetric characteristics of 6 and 10MV unflattened photon beams. *Radiother Oncol, 93: 141-146*.
18. Javedan K, Feygelman V, Zhang RR, Moros EG, Correa CR, Trotti A, *et al.* (2014) Monte Carlo comparison of superficial dose between flattening filter free and flattened beams. *Phys Med, 30: 503-508*.
19. Lee PC (1997) Monte Carlo simulations of the differential beam hardening effect of a flattening filter on a therapeutic X-ray beam. *Med Phys, 24: 1485-1489*.
20. Zefkili S, Kappas C, Rosenwald JC (1994) On-axis and off-

Int. J. Radiat. Res., Vol. 17 No. 1, January 2019

145

axis primary dose component in high energy photon beams. *Med Phys,* **21:** 799-808.

21. Sixel KE and Faddegon BA (1995) Calculation of X-ray spectra for radiosurgical beams. *Medical Physics, 22:* 1657 -1661.

22. Guillermineta C, Duvergera E, Gschwinda R, Makovickaa L, Monnierb A, Hamonb F, *et al.* (2001) Theoretical and experimental study of spectral distortions atthe output of an accelerator for medical use. *Radiat Phys Chem, 61:* 611– 613.

23. Walter LS (2002) Monte Carlo N-Particle transport code system for multiparticle and high energy applications LANL (Los Alamos National Laboratory), version 2.4.0, Ref Type: Serial (Book, Monograph).

24. Allahverdi M, Zabihzadeh M, Ay MR, Mahdavi SR, Shahriari M, Mesbahi A, *et al.* (2011) Monte Carlo estimation of electron contamination in a 18 MV clinical photon beam. *Int J Radiat Res, 9:* 15-28.

25. Zabihzadeh M, Shakarami Z, Birgani M, Shahbazian S, Behrooz MA (2015) Calculation of organs doses and secondary cancer risk during mantle field radiotherapy for Hodgkin's lymphoma. *Biosci Biotechnol Res Asia, 12:* 71-77.

26. Vassiliev ON, Titt U, Kry SF, Ponisch F, Gillin MT, Mohan R (2006) Monte Carlo study of photon fields from a flattening filter-free clinical accelerator. *Med Phys, 33:* 820-827.

27. Sheikh-Bagheri D and Rogers D (2002) Monte Carlo calculation of nine megavoltage photon beam spectra using the BEAM code. *Med Phys, 29:* 391-402.

28. Kajaria A, Sharma N, Sharma S, Pradhan S, Mandal A, Aggarwal LM (2016) Study of the dosimetric properties of an unflattened 6-MV photon beam by using the BEAMnrc code. *J Korean Phys Soc, 69:* 657-665.

29. Najem M, Spyrou N, Podolyák Z, Abolaban F (2014) The physical characteristics of the 15MV Varian Clinac 2100C unflattened beam. *Radiat Phys Chem, 95:* 205-209.

30. Day M and Aird E (1996) Central axis depth dose data for use in radiotherapy. *Br J Radiol, 25:* 138-151.

31. Wang Y, Khan MK, Ting JY, Easterling SB (2012) Surface dose investigation of the flattening filter-free photon beams. *Int J Radiat Oncol Biol Phys, 83:* 281-285.

32. Cashmore J (2016) Surface dose variations in 6 and 10 MV flattened and flattening filter-free (FFF) photon beams. *J Appl Clin Med Phys, 17:* 1-15.

33. Vassiliev ON, Titt U, Kry SF, Pönisch F, Gillin MT, Mohan R (2006) Dosimetric properties of photon beams from a flattening filter free clinical accelerator. *Med Phys, 33:* 820 -827.

146

Int. J. Radiat. Res., Vol. 17 No. 1, January 2019